Available online at www.sciencedirect.com
SCIENCE DIRECT®
Journal of APPLIED MATHEMATICS AND MECHANICS
ELSEVIER
www.elsevier.com/locate/jappmathmech
Journal of Applied Mathematics and Mechanics 69 (2005) 575–584

REGULAR AND CHAOTIC DYNAMICS OF A SPHERICAL BUBBLE†

I. Sh. AKHATOV and S. I. KONOVALOVA

North Dakota, USA and Ufa

e-mail: iskander.akhatov@ndsu.nodak.edu
sveta@imech.anrb.ru

(*Received* 13 *March* 2003)

The problem of the translational motion and oscillations of the radius of a spherical gas bubble in a spherical flask filled with a weakly compressible liquid is considered when there is forced radial perturbation of the flask wall. The translational motion is that of the bubble under the action of an acoustic field when there is viscous drag and the effect of added mass. A system of differential equations is proposed which describes the combined oscillations of the radius and the translational motion of the bubble. This system includes an ordinary differential equation of the Herring–Flinn–Gilmore type which describes the evolution of the radius of the bubble. Bifurcation diagrams are constructed for the radius of the bubble, which reveal a repeating structure of the bifurcation set within the limits of the harmonic resonances of the system. The dynamic characteristics of the bubble for different equilibrium radii are investigated numerically in connection with the analysis of the stability of its position in space.

The dynamics of cavitation bubbles in an acoustic field include both the oscillations of the radius of a bubble and the translational motion, that is, the displacement of the bubble in space. In a sufficiently strong acoustic field, cavitation bubbles oscillate in a non-linear manner and are one of the typical systems in which deterministic chaos manifests itself [1–3]. The non-linear aspects of the radial oscillations of the bubble surface have been investigated in many papers. The forced non-linear oscillations of a spherical gas bubble in an incompressible viscous liquid, subjected to the action of an acoustic field with different amplitudes of the pressure and frequencies, comparable with the resonance frequencies of the bubbles, have been investigated numerically in [4]. The results were presented in the form of resonance curves which show the dependence of the maximum radius of the bubble on the frequency of the acoustics field. It was formed that, in the case of an equilibrium radius $R_0 = 10$ μm and at pressure amplitudes exceeding the static Blake threshold ($P_b = 0.997$ atm), discontinuous transitions occur between the possible resonance, there is a gradual breakdown of the harmonics and they are replaced by ultraharmonics. As a result of the investigation of the non-linear oscillations of a bubble of fixed equilibrium radius using the methods of chaotic dynamics, it has been shown that the transition to chaotic oscillations and the return to regular oscillations occurs by means of forward and reverse bifurcations of a doubling of the period, and also by means of tangential (saddle-nodal) bifurcations and that the domains in which strange attractors arise become larger when the amplitude of the pressure of the acoustic field increases [5, 6]. Resonance curves showing the dependence of the maximum bubble radius on its equilibrium radius have been investigated for different pressure amplitudes in [7]. The resonance curves bear a resemblance both to the resonance curves obtained earlier in [4] and the bifurcation diagrams in [5]. It has been shown that, at sufficiently high amplitudes of the acoustic field pressure ($P_a > 1.2$ atm), a so-called "giant response" is initiated in the range of micron bubbles, when the bubble radius increases by an order or more in the oscillation process [7–9]. In all the above-mentioned papers, it is assumed that the bubble is located in an unbounded volume of liquid; the translation motion of the bubble was not considered.

†*Prikl. Mat. Mekh.* Vol. 69, No. 4, pp. 636–647, 2005.
0021–8928/$—see front matter.
doi: 10.1016/j.jappmathmech.2005.07.007

While the radial oscillations of the surface of a single bubble have been actively investigated by many researchers, less attention has been paid to the translational motion of the bubble. Nevertheless, nonlinear effects can also occur in the translational motion and the investigation of the positional stability of a bubble is therefore an important problem, especially when simulating the phenomenon of sonoluminescence when a bubble is subjected to the action of an intense acoustic field. For instance, an experimental investigation of the bubble dynamics in a travelling acoustic wave shows that a bubble with an equilibrium radius $R_0 \approx 50$ μm executes a chaotic zigzag-like motion in the direction in which the acoustic field varies if the sound intensity is sufficiently high ($I = 59$ μW/cm^2, $f = 70$ kHz) [10]. An unstable "dancing" motion of a bubble has also been experimentally recorded in a standing acoustic wave [11]. One of the possible mechanisms for the occurrence of "dancing" motion of a bubble is based on the assumption of a distortion of its spherical shape [11–13]. The translational motion of a spherical bubble, close to its resonance size, in the field of a standing acoustic wave has been investigated numerically in [14]. The Rayleigh–Lamb–Plesset equation for an incompressible liquid was used to describe the oscillatory motion [15–17]. It has been shown that a bubble with an equilibrium radius somewhat smaller than its resonance radius executes both chaotic radial motion and chaotic translational motion, Later, in [18], the Herring–Flinn–Gilmore equation [19], which takes account of the compressibility of the liquid, was used to describe the oscillatory motion. Non-chaotic but periodic motion of the bubble occurred for the same equilibrium radii. Hence, sufficient attenuation for the development of stable solutions is ensured by the compressibility of the liquid.

Below we present a numerical investigation of the dynamics of a gas bubble, which is somewhat smaller than its own resonance size, executing both radial oscillations and translational motion in a spherical flask filled with a viscous weakly compressible liquid in which a standing acoustic wave with an amplitude $P_a = 1.8$ and a frequency $f = 20$ kHz is formed. It is assumed that the spherical shape of the bubble is not distorted.

1. FORMULATION OF THE PROBLEM

We consider a spherical flask filled with a viscous weakly compressible liquid in which an acoustic wave is created in the form of a spherical standing wave. We will assume that the antinode of the acoustic wave is located at the centre of the flask and that the closest nodes are on its boundary. Such a simplified formulation of the problem is often used when simulating the dynamics of a single bubble [20–24]. The acoustic pressure distribution in the liquid, which is a solution of the linear wave equation for a weakly compressible liquid, can be represented in the form

$$p(r, t) = P_0 + p_a \frac{\sin kr}{kr}$$

where r is the translational coordinate, t is the time, P_0 is the atmospheric pressure, $p_a = -P_a \sin\omega t$ is the acoustic pressure at the centre of the flask with amplitude P_a, $k = \omega/c$ is the wave number, c is the velocity of sound in the liquid and ω is the angular frequency of the acoustic wave.

The corresponding velocity field in the liquid is given by the formula

$$\mathbf{v}_l = v_l \mathbf{e}_r = -\frac{P_a}{\rho_l \omega} \cos\omega t \left(\frac{\cos kr}{r} - \frac{\sin kr}{kr^2} \right) \mathbf{e}_r$$

where $\mathbf{e}_r$ is the unit vector in the radial direction, ρ_l is the density and v_l is the velocity of the liquid.

2. MATHEMATICAL MODEL

In order to simulate the evolution of the bubble radius, models of the spherically symmetric oscillations of the surface of a single bubble in an unbounded volume of both an incompressible liquid (the Rayleigh–Lamb–Plesset equation) and a weakly compressible liquid (the Herring–Flinn–Gilmore equation) and models similar to these are conventionally used [25, 26]. In the case of a bounded volume of liquid, a mathematical model is used which describes the radial oscillations of the bubble surface in a spherical flask filled with a weakly compressible liquid when the flask walls serve as the source of the perturbation of the oscillations in the liquid [22–24]. It includes an ordinary differential equation which is analogous to the Herring–Flinn–Gilmore equation and an equation with a delay which relates the pressure on the flask walls to the change in the bubble radius. In this paper, it is assumed that the

oscillations of the bubble have no effect on the acoustic pressure distribution in the liquid and the radial oscillations of the bubble are therefore modelled by a Herring–Flinn–Gilmore equation in the form

$$\left(1-\frac{\dot{R}}{c}\right)R\ddot{R}+\frac{3}{2}\dot{R}^2\left(1-\frac{\dot{R}}{3c}\right)=\left(1+\frac{\dot{R}}{c}\right)\frac{p_w-p(r,t)}{\rho_l}+\frac{R}{\rho_l c}\frac{d}{dt}(p_w-p(r,t)) \tag{2.1}$$

Here $R = R(t)$ is the variable bubble radius and p_w is the pressure in the liquid close to the bubble surface. Assuming that the gas in the bubble expands adiabatically and neglecting the vapour pressure in the bubble, the pressure in the liquid close to the bubble surface can be represented in the form

$$p_w=\left(P_0+\frac{2\sigma}{R_0}\right)\left(\frac{R_0}{R}\right)^{3\gamma}-\frac{2\sigma}{R}-\frac{4\mu\dot{R}}{R}$$

where R_0 is the equilibrium bubble radius, σ is the surface tension coefficient, γ is the adiabatic exponent and μ is the viscosity of the liquid.

The translational motion is the progressive motion of the bubble under the action of the variable acoustic and gravitational fields when there is fluid drag and the added effect mass

$$\frac{4}{3}\pi R_0^3\rho_g\dot{\mathbf{v}}_b=\mathbf{F}_g+\mathbf{F}_b+\mathbf{F}_m+\mathbf{F}_s \tag{2.2}$$

where ρ_g is the density of the gas in the unperturbed bubble, $\mathbf{v}_b$ is the bubble velocity, $\mathbf{F}_g$ is the flotation force, $\mathbf{F}_b$ is the Bjerknes force, which acts as viewed from the acoustic wave and causes the bubble to be attracted to the antinode or node of the wave of the acoustic field, $\mathbf{F}_m$ is the force due to the added masse effect and $\mathbf{F}_s$ is the viscous drag.

The flotation force. We define the flotation force as the sum of the gravity force and the buoyancy force

$$\mathbf{F}_g=-\frac{4}{3}\pi R^3\left[\rho_l-\left(\frac{R_0}{R}\right)^3\rho_g\right]\mathbf{g} \tag{2.3}$$

where g is the acceleration due to gravity.

The Bjerknes force. It is well known that a force $\mathbf{F} = -V\nabla p$ acts on a body of volume V in a liquid with a pressure gradient ∇p. The force F, which is usually averaged over time, is called the Bjerknes force. In this paper, the motion of bubbles is investigated in the time scale in which the acoustic field varies. We therefore define the Bjerknes force as the instantaneous magnitude of this force

$$\mathbf{F}_b=-\frac{4}{3}\pi R^3\nabla p(r,t)=\frac{4}{3}\pi R^3\rho_l\dot{\mathbf{v}}_l \tag{2.4}$$

Note that the Bjerknes force and the buoyancy force are of the same nature: both forces are due to a pressure gradient or a difference in pressure on the opposite walls of a bubble. However, in the case of the buoyancy force, this is a gradient in the hydrostatic pressure $\rho_l\mathbf{g}$ while, in the case of the Bjerknes force, it is the acoustic pressure gradient. It is for this reason that the Bjerknes force is sometimes referred to as the acoustic force of buoyancy.

The force due to the added effect mass. Assuming that there is a potential flow of the compressible liquid around the bubble, we write the additional momentum of the liquid which is set into motion by the bubble in the form

$$\mathbf{P}=\frac{1}{2}V_b\rho_l(\mathbf{v}_b-\mathbf{v}_l)$$

where V_b is the bubble volume. The change in this momentum with time leads to the appearance of an additional force of reaction which acts on the bubble.

$$\mathbf{F}_m=-\frac{1}{2}\frac{d}{dt}\left(\frac{4}{3}\pi R^3\rho_l(\mathbf{v}_b-\mathbf{v}_l)\right) \tag{2.5}$$

The viscous drag force. As viewed from the liquid, a drag force, which is due to the viscosity of the liquid, acts on a moving bubble. At low Reynolds numbers ($\mathrm{Re} = 2R\rho_l|\mathbf{v}_l - \mathbf{v}_b|/\mu \ll 1$), neglecting the viscosity of the gas within the bubble compared with the viscosity of the liquid surrounding it, this force is equal to (see, for example, [17, 27])

$$\mathbf{F}_s = 4\pi\mu R(\mathbf{v}_l - \mathbf{v}_b) \tag{2.6}$$

Substituting the expressions for the forces (2.3)–(2.6) into Eq. (2.2), we obtain the vector differential equation for the bubble velocity

$$\dot{\mathbf{v}}_b = \left(\frac{1}{3} + \alpha\right)^{-1}\left[\dot{\mathbf{v}}_l + \left(\frac{\dot{R}}{R} + 2\frac{\nu}{R^2}\right)(\mathbf{v}_l - \mathbf{v}_b) - \left(\frac{2}{3} - \alpha\right)\mathbf{g}\right], \quad \alpha = \frac{2}{3}\frac{\rho_g}{\rho_l}\left(\frac{R_0}{R}\right)^3 \tag{2.7}$$

where $\nu = \mu/\rho_l$ is the kinematic viscosity of the liquid.

A similar equation has been used by a number of researchers ([14, 28] and others) to solve problems associated with the motion of bubbles.

In a polar system of coordinates (r, θ) with the pole at the centre of the flask, Eq. (2.7) reduces to the following system of scalar equations

$$\begin{aligned} \ddot{r} &= r\dot{\theta}^2 + \left(\frac{1}{3} + \alpha\right)^{-1}\left[\dot{v}_l + \left(\frac{\dot{R}}{R} + 2\frac{\nu}{R^2}\right)(v_l - \dot{r}) + \left(\frac{2}{3} - \alpha\right)g\sin\theta\right] \\ \ddot{\theta} &= -2\frac{\dot{r}}{r}\dot{\theta} - \left(\frac{1}{3} + \alpha\right)^{-1}\left[\left(\frac{\dot{R}}{R} + 2\frac{\nu}{R^2}\right)\dot{\theta} + \left(\frac{2}{3} - \alpha\right)g\frac{\cos\theta}{r}\right] \end{aligned} \tag{2.8}$$

3. RESULTS OF NUMERICAL CALCULATIONS

The system of non-linear differential equations (2.1), (2.8), which describes the combined radial oscillations and translational motion of a bubble, was investigated numerically. A fifth-order Runge–Kutta method was used, which enables one to select the length of the step automatically, such that the local error does not exceed a prescribed acceptable value [29]. This property of the method is particularly important since, at the instant when collapse occurs, it takes place very rapidly. Calculations were carried out for the following values of the physical parameters: $P_0 = 1$ atm, $P_a = 1.8$ atm, $\omega = 2\pi \times 20$ kHz, $c = 1500$ m s^{-1}, $\rho_l = 998$ kg m^{-3}, $\rho_g = 1$ kg m^{-3}, $\sigma = 0.0725$ N m^{-1}, $\mu = 10^{-3}$ kg m^{-1} s^{-1}, $\gamma = 1.4$ and $g = 9.8$ m s^{-2}.

The direction of the translational motion of the bubble is determined by the Bjerknes and buoyancy forces. Translational motion is a radial direction is caused by the Bjerknes force, which is larger than the buoyancy force by two orders of magnitude. A bubble can be repelled from the antinode ($\mathbf{F}_b|_r > 0$) or attracted to it ($\mathbf{F}_b|_r < 0$) depending on the equilibrium radius R_0 and the radial translational coordinate r. Since $\mathbf{F}_b|_\theta = 0$, the bubble motion in a polar direction is solely determined by the buoyancy force. The polar translational coordinate $\theta(t)$ increases monotically: $\theta \to \pi/2$. This means that the bubble approaches the vertical axis, passing through the antinode of the acoustic field.

A diagram of the directions of the averaged Bjerknes force for a bubble when an equilibrium radius R_0 and a translational coordinate r is shown in Fig. 1(a). Calculations of the Bjerknes force, averaged over the period of the acoustic field, were carried out for a fixed bubble when $5 \le R_0 \le 45$ μm and $4 \le r \le 16$ mm. The range of values of (R_0, r) for which $\mathbf{F}_b|_r > 0$ is denoted by a grey colour and the range of values for which $\mathbf{F}_b|_r < 0$ is denoted by a white colour. So, a bubble with $R_0 = 15$ μm can be attracted to the antinode when $r(t)|_{t=0} > 7.5$ mm. If, however, $r(t)|_{t=0} < 7.5$ mm, the bubble will be replaced from the antinode and move towards the node. In any case, if occupies a stable position on the boundary of the domains attraction and repulsion at a distance of $r \approx 7.5$ mm from the antinode. Actually, the oscillations of the bubble radius induce high-frequency oscillations about its stable position with a period of the acoustic field. $T = 50$ and an amplitude of the order of 10 μm, which is comparable with the bubble size. A solution of this type can be called a quasistationary solution.

The form of the steady translational motion of a bubble with initial coordinates (7.5 mm, $\pi/3$) is also in Fig. 1(a). The time relaxation was taken to be equal to 500 periods of the acoustic field. The calculated maximum and minimum values of $r(t)$ for each $R_0 \in [5, 45]$ μm after 200 periods of the acoustic wave are shown by the solid curves. The local maxima, corresponding to harmonic resonance of the bubble radius, are denoted by the points. In the case R_0, at which the curves $r_{\max}(R_0)$ and $r_{\min}(R_0)$ coincide,

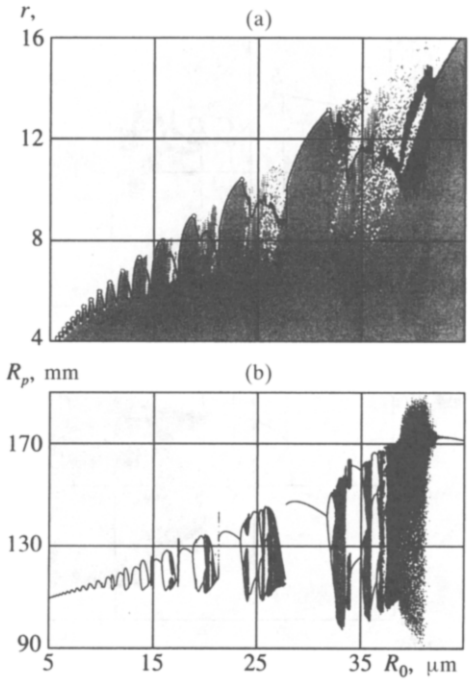

Fig. 1

a quasistationary solution is obtained for the translational coordinate. High-frequency, low-amplitude oscillations of the bubble are not seen on the scale used for the diagram. Here, the curves also coincide with the boundary between the domains of attraction and repulsion. In the case of R_0, for which no sharp boundary is traced between the domains of attraction and repulsion, the curves $r_{max}(R_0)$ and $r_{min}(R_0)$ do not coincide. This means that the bubble performs chaotic low-frequency oscillations in a radial direction with an amplitude which is, on average, two orders of magnitude greater than the amplitude of the high-frequency oscillations.

The bifurcation diagram for the bubble radius is shown in Fig. 1(b). A hundred values of the bubble radius $R(t)$ were established corresponding to each value of the control parameter R_0 at successive instants of time of the steady motion of the bubble $t = nT$. The set of values of $R_p = R(t)$, $t = nT$ is one of the projections of a Poincaré section. In cases when all the points are superimposed on one another, the attractor (the attractive trajectory in phase space) is the limit cycle of a single period. This means that the period of the oscillatory motion of the bubble is equal to T. When the control parameter is changed, the system can escape from a stable state and bifurcation occurs with a qualitative change in the character of the process. If the non-linearity, which is inherent to the system, is such that the perturbation changes sign at the threshold of loss of stability during a single circuit of the limit cycle then, in order for the trajectory to be closed, it is necessary to perform a further circuit so that the period of the motion which has arisen is again twice as large as the period of the initial motion. The birth of a cycle with a period which is twice as great as the initial cycle will be the result of bifurcation. This is period-doubling bifurcation. Very often, bifurcations of the same nature follow again after it, if there is a further change in the parameter. The sequence of bifurcation values of the parameter accumulates to a definite limit, the critical point, which is the boundary of chaos. The transition to chaos through a cascade of bifurcations involving a period-doubling bifurcation is the Feigenbaum scenario [30].

Another situation may be encountered when, as a bifurcation point is approached, an unstable cycle approaches a stable limit cycle and, at the bifurcation point, the two cycles merge and disappear. Hence, no stable periodic orbits at all remain in the domain of the phase space being considered. This is inverse tangential or saddle-nodal bifurcation. The opening in the chaotic system of period 3 in Fig. 2(c) when the tangential bifurcation when $R_0 \approx 33.5$ μm generates a stable cycle of period 3 and an unstable cycle of period 3 (not shown in the figure) serves as a simple example. It should be noted that tangential bifurcations are characteristic of the Feigenbaum scenario and represent a unique mechanism by which a cycle of odd period (unlike a period-doubling bifurcation) can appear. The windows in the chaotic system of period 3 and 4, which are generated by tangential bifurcations, are seen in Fig. 1(b) within the limits of the last three harmonics.

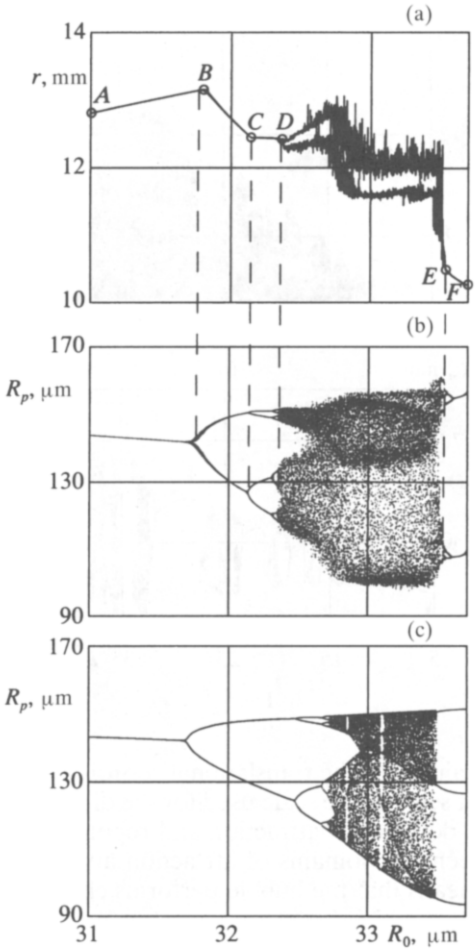

Fig. 2

A similarity of sections of the bifurcation diagram is observed within the limits of the harmonic resonances: successive period-doubling bifurcations occur which lead to chaotic oscillations of the bubble radius and the return to periodic oscillations through inverse period-doubling bifurcations and tangential (saddle-nodal) bifurcations. As R_0 increase, the pattern becomes more complicated and the domains of chaotic oscillations of the bubble radius expand but the similarity of the curves is preserved. The translational characteristic $r(t)$ also preserves an analogous similarity within the limits of the harmonic resonances.

The link between the translational and radial characteristics of the bubble is clearly seen in Fig. 2 for $R_0 \in [31, 33.75]$ μm. A quasistationary solution for the translational coordinate $r(t)$ is obtained in the section $ABCD$ of Fig. 2(a). Point B corresponds to the first period-doubling bifurcation of the oscillations of the bubble radius. A second bifurcation occurs at the point C and, at the critical point D, there is both a transition to chaotic oscillations of the radius as well as a change in the form of the translational coordinate from a quasistationary form to a chaotic form. The curves r_{max} and r_{min} become irregular in the section DE and the amplitude of the chaotic translational oscillations (about 1 mm) is large compared with the quasistationary case. At point E, there is a return to a quasistationary solution for the translational coordinate $r(t)$ and periodic oscillations of the radius. Regular dynamics of the bubble occur in the section EF. A quasistationary solution for the translational coordinate is therefore obtained for values of R_0 at which periodic oscillations of the bubble radius are observed: in cases when these oscillations become chaotic, the translation coordinate also changes in an irregular manner.

The bifurcation diagram, ignoring the translational motion of the bubble, at a fixed distance $r = 13$ mm from the antinode, is shown in Fig. 2(c). It is seen that the transition to chaos takes place according to the Feigenbaum scenario. In Fig. 2(b), the fine structure of the bifurcations is blurred on account of the existence of translational motion.

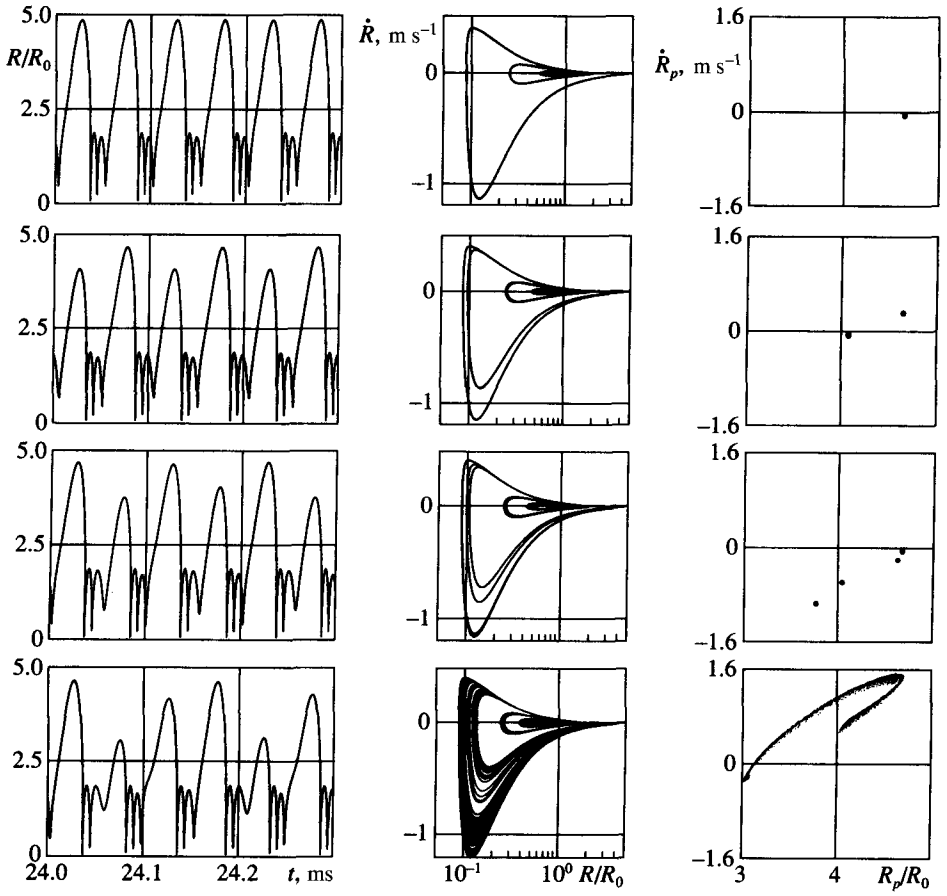

Fig. 3

The transition to chaos in the section $R_0 \in [31, 33]$ is illustrated in Fig. 3. The oscillations of the bubble radius are shown in the left-hand column, the phase trajectories in the middle column and the Poincaré sections in the right-hand column. Starting from the top, the radial characteristics are shown for $R_0 = 31$ μm (from section AB in Fig. 2a and b), $R_0 = 32$ μm (from section BC), $R_0 = 32.3$ μm (from section CD) and $R_0 = 33$ μm (from section DE). In the first series, the period of the oscillations of the bubble radius is equal to the period of the acoustic field T. The attractor is the limit cycle of period T and all of the points of intersection with the phase trajectory are superimposed on one another since R_p/R_0 and $\dot{R}_p$ take the same values over the period T and the Poincaré section consists of a single point. In the second series, the oscillations of the bubble radius are repeated over two periods of the acoustic field. The phase trajectory is the limit cycle of period $2T$ which corresponds to the appearance of a further point in the Poincaré section: a period-doubling occurs. In the third series, a subsequent period-doubling bifurcation is demonstrated, which leads to the birth of a limit cycle of period $4T$. The oscillations of the bubble radius in the bottom series have a chaotic character and the phase trajectory is a strange attractor, the structure of which is also traced in the Poincaré section where no two points coincide.

The change in the translational coordinate in the course of prolonged action of the acoustic field is shown in Figs 4(a and b) in order to illustrate the chaotic "dancing" motion of the bubble when $R_0 = 33$ μm and $R_0 = 40$ μm from the two windows of irregular change in the translational coordinate ($R_0 \in [32.4, 33.5]$ μm and $R_0 \in [37.5, 42]$ μm, see Fig. 1a and 2a). Chaotic oscillations of the bubble radius correspond to these regions of the parameter R_0 (see Figs 1b and 2b). It can be seen that the amplitude of the envelope of the translational coordinate $r(t)$ can reach 3.5 mm.

Besides the chaotic motion, a periodic "dancing" motion of the bubble was also observed. Figure 5 shows the four regions of variations of the parameter R_0 ("windows of periodicity") in which low-frequency quasiperiodic solution $r(t)$ are obtained, and the sections of the bifurcation diagram for the bubble radius corresponding to them. Note that there is a similarity in the sections of the curves for

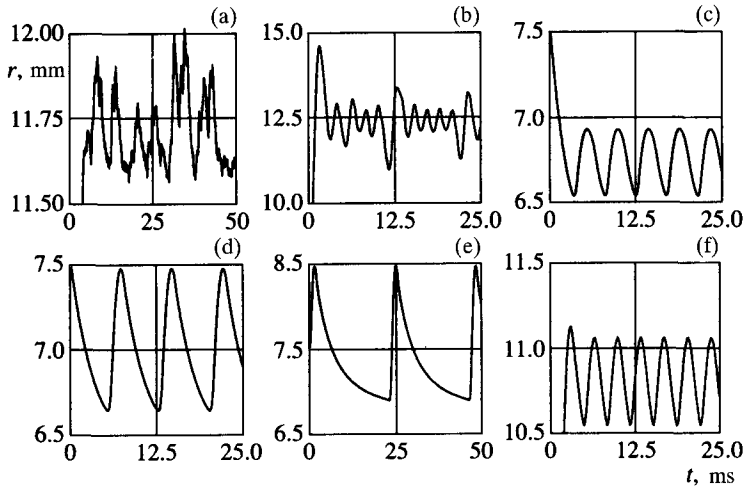

Fig. 4

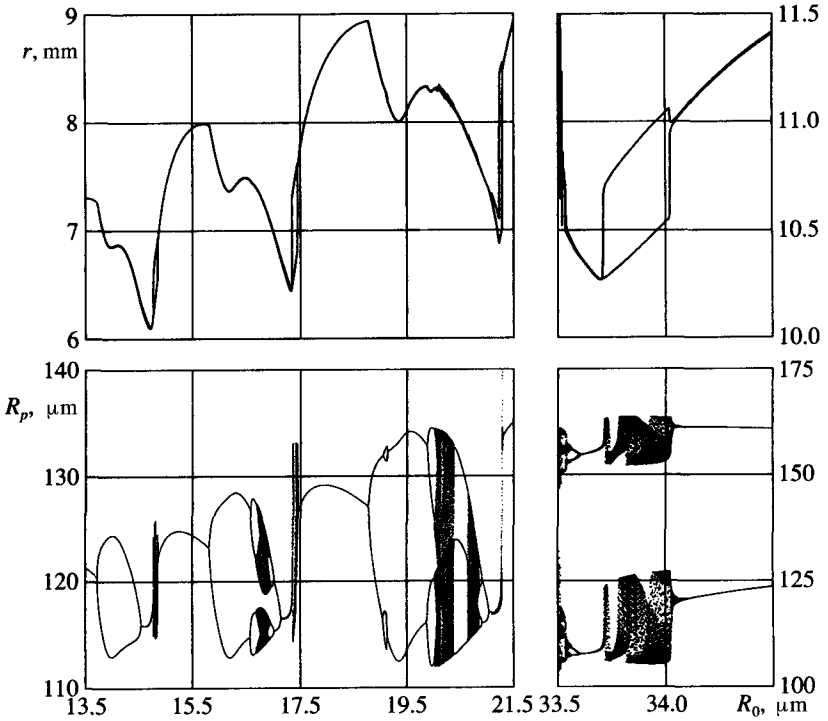

Fig. 5

the translational and radial characteristics within the limits of the harmonic resonances. In the bifurcation diagram for the bubble radius, windows of chaotic radial oscillations, which emerge in the boundary laminar regions between the harmonic resonances, correspond to the "windows of periodicity".

The change in the translational coordinate of the bubble is shown in Fig. 4(c–f) for each of the four regions for R_0 = 14.8, 17.4, 21.2, 34.0 μm respectively. The maximum amplitude of the envelope of the translational coordinate ($A_{mod} = r_{max} - r_{min}$ = 1.6 mm) and the period of the low-frequency modulation (T_{mod} = 24 ms, $T_{mod} \approx 500 \times T$) is observed when $R_0 \in$ [21.1, 21.3] μm. The principal characteristics of the "dancing" motion of the bubble are presented in Table 1.

Table 1

	Chaotic motion		Periodic motion			
R_0, μm	32.4–33.5	37.5–42	14.77–14.86	17.35–17.46	21.1–21.3	33.7–34
A_{mod}, mm	0.5	3.5	0.4	0.8	1.6	0.5
T_{mod}, ms	–	2	4.5	8	24	3.5

Note that, as the equilibrium radius increases, the "windows of periodicity" which emerge become wider. Furthermore, the amplitude and period of the oscillations of the envelope of the translational coordinate of the bubble from each successive "window of periodicity" (apart from the last one when $R_0 \in [33.7, 34]$) also become larger.

4. CONCLUSION

The bifurcation diagrams constructed for the radius of the bubble as a function of its equilibrium radius show that, within the limits of the harmonic resonance, the transition to chaotic oscillations and the return to periodic oscillations occur in accordance with the Feigenbaum scenario. There is therefore a similarity in the sections of the bifurcation diagrams in the regions of harmonic resonance and, as the equilibrium radius becomes larger, cascades of bifurcations are initiated and the regions of chaotic oscillations grow.

The translational characteristic also preserves an analogous similarity. It has been shown that there are three modes for the translational coordinate, depending on the form of the radial oscillations: quasistationary, quasiperiodic and chaotic. On the other hand, the form of the radial oscillations is determined not only by the equilibrium radius of the bubble but, also, by its position in space. Hence, when investigating bubble dynamics, it is not sufficient to consider merely the radial oscillations of its surface; it is also necessary to take account of the displacement of the bubble in space.

A quasistationary mode is obtained for those equilibrium radii for which the oscillations of the bubble are periodic with period T, $2T$ and so on. In the same place where the radial oscillations are chaotic, translational coordinate changes in an irregular manner and a chaotic "dancing" motion of the bubble occurs, during which the amplitude of the translational coordinate envelope can reach 3.5 mm. Apart from the chaotic "dancing" motion of the bubble, a quasiperiodic translational motion also occurs for certain equilibrium radii which is the superposition of regular low-frequency oscillations of sufficiently large amplitude with high-frequency oscillations of small amplitude. In the bifurcation diagram for the bubble radius, the windows of chaotic radial oscillations, which arise in the boundary laminar regions between the harmonic resonances when $R_0 > 13$ μm, correspond to "windows of periodicity".

At the same time, the maximum amplitude of the envelope of the translational coordinate $A_{mod} = 16$ and the maximum period of the low-frequency modulation $T_{mod} = 24$ ms ($T_{mod} \approx 500 \times T$) are observed when $R_0 \in [21.1, 21.3]$ μm.

The result obtained can be interpreted as a possible mechanism for the occurrence of chaotic "dancing" motion of a bubble, which does not assume a breakdown of the spherical form of the bubble.

This research was supported financially by the Russian Foundation for Basic Research (02-01-97912).

REFERENCES

1. LAUTERBORN, W., PARLITZ, U., HOLZFUSS, J., BILLO, A. and AKHATOV, I., Acoustic chaos. *Chaotic, Fractal, and Nonlinear Signal Processing: Proc. 3rd Techn. Conf. Nonlinear Dynamics (Chaos) and Full Spectrum Processing*. Mystic, Connecticut, USA, 1995 (Edited by Katz, R. A.). Woodbury, New York, 1996, Vol. 375.
2. LAUTERBORN, W., *Cavitation. Encyclopedia of Acoustics* (Edited by Crocked, M. J.). Wiley, New York, 1997, Vol. 1, 263–270.
3. LAUTERBORN, W., KURZ, T. and PARLITZ, U., Experimental nonlinear physics. *Intern. J. Bifurc. Chaos*, 1997, **7**, 9–10, 2003–2033.
4. LAUTERBORN, W., Numerical investigation of nonlinear oscillations of gas bubbles in liquids. *J. Acoust. Soc. America*, 1976, **59**, 2, 283–293.
5. PARLITZ, U., ENGLISCH, V., SCHEFFCZYK, C. and LAUTERBORN, W., Bifurcation structure of bubble oscillators. *J. Acoust. Soc. America*, 1990, **88**, 2, 1061–1077.
6. LAUTERBORN, W. and PARLITZ, U., Methods of chaos physics and their application to acoustic. *J. Acoust. Soc. America*, 1988, **84**, 6, 1975–1993.
7. LAUTERBORN, W. and METTIN, R., Nonlinear bubble dynamics: response curves and more. *Sonochemistry and Sonoluminescence* (Edited by Crum, L. A, *et al.*). Kluwer, Dordrecht, 1999, 63–72.

8. AKHATOV, I., GUMEROV, N., OHL, C. D., PARLITZ, U. and LAUTERBORN, W., The role of surface tension in stable single-bubble sonoluminescence. *Phys. Rev. Lett.* 1997, **78**, 2, 227–230.
9. AKHATOV, I., OHL, C. D., METTIN, R. and LAUTERBORN, W., Giant response in dynamics of small bubbles. *Proc. 16th Intern. Congr. Acoustics and 135th Meeting of the ASA*, Seattle, 1998, 2285–2286.
10. YOSIOKA, K., KAWASIMA, Y. and HIRANO, H., Acoustic radiation pressure on bubbles and their logarithmic decrement. *Acustica*, 1955, **5**, 3, 173–178.
11. ELLER, A. I. and CRUM, L. A., Instability of the emotion of a pulsating bubble in a sound field, *J. Acoust. Soc. America*, 1970, **47**, 3, Part 2, 762–767.
12. BENJAMIN, T. B. and ELLIS, A. T., Self-propulsion of asymmetrically vibrating bubbles. *J. Fluid Mech.*, 1990, **212**, 65–80.
13. ZARDI, D. and SEMINARA, G., Chaotic mode competition in the shape oscillations of pulsating bubbles. *J. Fluid Mech.*, 1995, 286, 257–276.
14. WATANABE, T. and KUKITA, Y., Translational and radial motions of a bubble in an acoustic standing wave field. *Phys. Fluids A*, 1993, **5**, 11, 2682–2688.
15. RAYLEIGH, LORD., On the pressure developed in a liquid during the collapse of a spherical cavity. *Phil. Mag.*, 1917, **34**, 200, 94–97.
16. LAMB, H., *Hydrodynamics*. University Press, Cambridge, 1924.
17. NIGMATULIN, R. I., *Dynamics of Multiphase Media*. Vol. 1. Nauka, Moscow, 1987.
18. CORDRY, S. M., Bjerknes forces and temperature effects in single-bubble sonoluminescence. PhD Thesis. The University of Mississippi, 1995.
19. KNAPP, R. T., DAILY, J. W. and HAMMIT, F. G., *Cavitation*. McGraw-Hill, New York, 1970.
20. AKHATOV, I., METTIN, R., OHL, C. D., PARLITZ, U. and LAUTERBORN, W., Bjerknes force threshold for stable single bubble sonoluminescense. *Phys. Rev. E.*, 1997, **55**, 3, 3747–3750.
21. METTIN, R., AKHATOV, I., PARLITZ, U., OHL, C. D. and LAUTERBORN, W., Bjerknes forces between small cavitation bubbles in a strong acoustic field. *Phys. Rev. E.*, 1997, **56**, 3, 2924–2931.
22. AKHATOV, I. Sh., VAKHIMOVA, N. K., GALEYEVA, G. Ya., NIGMATULIN, R. I. and KHISMATULLIN, D. B., Weak oscillations of a gas bubble in a spherical volume of a compressible liquid. *Prikl. Mat. Mekh.*, 1997, **61**, 6, 695–962.
23. NIGMATULIN, R., AKHATOV, I., VAKHITOVA, N. and LAHEY, R., The resonant supercompression and sonoluminescence of a gas bubble in a liquid-filled flask. *Chem. Eng. Comm.*, 1998, **168**, 145–169.
24. NIGMATULIN, R., AKHATOV, I., VAKHITOVA, N. and LAHEY, R. T., On the forced oscillations of a small gas bubble in a spherical liquid-filled flask. *J. Fluid Mech.*, 2002, **414**, 47–73.
25. PROSPERETTI, A. and LEZZI, A., Bubble dynamics in a compressible liquid. 1. First-order theory. *J. Fluid Mech.*, 1986, **168**, 457–478.
26. LEZZI, A. and PROSPERETTI, A., Bubble dynamics in a compressible liquid. 2. Second-order theory. *J. Fluid Mech.*, 1987, **185**, 289–321.
27. LEVICH, V. G., *Physicochemical Hydrodynamics*. Prentice-Hall, Englewood Cliffs, NJ, 1962.
28. KAMEDA, M. and MATSUMOTO, Y., Shock waves in liquids containing small gas bubbles. *Phys. Fluids*, 1996, **8**, 2, 322–335.
29. HAIRER, E., NORSETT, S. P. and WANNER, G., *Solving Ordinary Differential Equations I. Nonstiff Problems.* Springer, Berlin, 1987.
30. SCHUSTER, H., *Deterministic Chaos. An Introduction*. Physik-Verlag, Weinheim, 1984.

Translated by E.L.S.